

ELECTRON-OPTICAL STUDY OF SMECTITES*

by

J. MERING and A. OBERLIN

École de Physique et Chimie Industrielles, rue Vauquelin, Paris V, France

and

Laboratoire de Minéralogie-Cristallographie, Faculté des Sciences,
1 rue Victor Cousin, Paris V, France

ABSTRACT

THE combined use of electron microscopy and of selected area diffraction (SAD) has been applied to the study of montmorillonites from Wyoming and from Camp-Berteaux, of nontronite, and of hectorite. The study shows that only the elementary layers of the Wyoming montmorillonite and of the nontronite are single two-dimensional crystals. The elementary layers of the montmorillonite from Camp-Berteaux are formed by edge-to-edge associations of very small elements with mutual orientations of about 60° or multiples of 60° . The layers of hectorite are formed by edge-to-edge association of laths with fluctuations of orientation of the order of 10° rotation around adjoining edges. The SAD patterns of Wyoming montmorillonite show that the single layer plane symmetry group of this mineral is $1\bar{1}1$; nontronite layers belong to the symmetry group $c2mm$. The study of thick particles shows that in turbostratic smectites the layers are stacked with mutual rotations around the perpendicular to their plane. This mode of stacking explains the absence of hkl reflections. High resolution diffraction (HRD) patterns obtained with sample inclined to the electron beam show that only the structure of hectorite approaches the ideal model; nontronite and montmorillonite exhibit appreciable distortions with respect to the ideal model. HRD diagrams provide precise information for the refinement of the crystal structures of smectites.

INTRODUCTION

ELECTRON-OPTICAL methods involve the combined use of the electron microscope and electron diffraction. Electron diffraction and X-ray diffraction methods are not identical, but are complementary to each other. The principal advantage of electron diffraction lies in the high diffracted intensity which allows observations to be made on material of very small volume. The method of selected area diffraction (SAD) allows one to obtain diffraction diagrams of single crystals with diameters of about 1000 \AA . In the method of high resolution diffraction (HRD) the incident beam covers a large sample surface, the thickness of which can be reduced to a few tens of angstroms; this allows one to work with very well-oriented deposits. The combined advantages of these techniques compensate for the main inconvenience of electron diffraction, namely the impossibility of studying hydrated states

* Translated from the original French by G. W. Brindley.

and limitations on the choice of the exchangeable cations (imposed by the necessity of having a suitable dispersion of the mineral).

Electron diffraction is particularly suitable for the study of smectites which are mainly minerals with a turbostratic structure; the interpretation of the results is simplified by the elimination, for example, of the risk of dynamic phenomena affecting the results. In a turbostratic mineral, X-ray diagrams show the $00l$ Bragg reflections together with characteristic asymmetric diffraction bands from the two-dimensional crystal lattices. The diffracted beams from different elementary layers, characterized by two indices, h and k (other than 00), cannot interfere coherently. There is no three-dimensional crystalline order. If one considers an elementary layer of a smectite with unit cell dimensions a and b , the structure in reciprocal space is reduced to a system of straight lines perpendicular to the plane of the sheet and passing through the points of the two-dimensional reciprocal lattice a^*b^* . Each line is characterized by two integral indices h and k while a point on a line is defined additionally by a distance Z measured from the origin plane (parallel to the plane of the crystalline sheet). Each of these points has a weight proportional to the diffracted intensity $|F_{hk}(Z)|^2$. As for all phyllites, the unit cell of the sheet, ab , is ortho-hexagonal with $b=a\sqrt{3}$. Consequently, several interferences are situated on the same circle and therefore can give rise to overlapping reflections. This overlap is always present in X-ray diagrams which are produced mainly from a mass of particles more or less strongly disoriented. Each asymmetric band observed in an X-ray diagram is a superposition of several bands with different indices, such as 02 , 11 . For this reason X-ray diffraction does not allow a choice to be made between various possible symmetry groups.

One sees immediately the value of using the SAD technique.

(i) With very thin particles, preferably reduced to a single elementary layer, the SAD technique gives a section orthogonal to the system of reciprocal lines in the neighborhood of $Z=0$. This limits the available information but gives the possibility of observing separately interferences related by pseudo-hexagonal symmetry, for example one observes separately the 11 , $1\bar{1}$, 02 reflections. This removes the indetermination of the symmetry group for dioctahedral smectites that is related to the three possible arrangements of the octahedral cations in the layer.

(ii) Any study of a colloidal system involves the problem of the shape and dimensions of the particles; several types can be considered:

(a) X-ray diffraction allows one to measure the layer dimensions of a smectite. The limits of the layers measured in this way are defined by a discontinuity of orientation; the disorientation can be very small. Particles defined by X-ray diffraction constitute what we may call *primary particles* (this is equivalent to the concept of a crystallite in two dimensions).

(b) Dispersion of the material in water presupposes the liberation of particles which we shall call *free particles*.

- (c) The elements of a suspension collected on a substrate and examined in an electron microscope constitute a third type of particle, an *aggregated particle*.

In practice there is no direct method for determining the dimensions of free particles in suspension. Particles seen in an electron microscope are generally larger than the primary particles determined by X-rays, and often are *edge-to-edge associations* of primary particles. It is likely that the same kind of association is produced between the free particles on a substrate. The combined use of the electron microscope and the SAD technique allows one to study the manner of association of the primary particles forming the visible particle seen in the microscope. By using techniques which tend to suppress the edge-to-edge association one may obtain a more precise idea of the diameter and the morphology of the free particle.

(iii) Observations made by the SAD technique on thick particles indicate the orientation of layers stacked on each other. Thick particles may be formed by sedimentation on to the substrate, or may pre-exist in a non-dispersed form in the initial suspension. In both cases they provide a picture of the turbostratic arrangement made evident by X-ray diffraction, and provide an explanation for the absence of coherent scattering by successive layers.

With the HRD method the advantage of separating reflections having the same hexagonal multiplicity is lost. The electron beam covers a surface of several hundreds of microns squared, and intercepts the two-dimensional layers turned at random around the perpendicular to their mean plane. However, it also allows one to utilize the very small thickness of the sample preparation which makes the particles lie with their (001) faces parallel within a few degrees. Such good orientation cannot be obtained with samples prepared for X-ray diffraction since their thickness should be about 0.01 mm and the disorientation of the (001) faces is then of the order of 20° .

With the sample perpendicular to the electron beam, HRD diagrams represent a perpendicular section in the region of $Z=0$ of the system of concentric cylinders generated by the rotation of the reciprocal lines hk around the reciprocal line 00 . The good orientation of the particles is recognized by the symmetrical profiles of the diffraction rings. The maxima of the rings enable one to measure directly the parameters a and b of the unit cell. A similar measurement using X-ray powder diagrams gives false results because of the asymmetry of the hk bands, and this affects even the band 06, 33 which is generally used for measuring the parameter b (Brindley and Mering, 1951).

Much more important, however, is the oblique diffraction pattern obtained when the sample is inclined at a considerable angle to the incident electron beam (Zvyagin, 1957). The diffraction diagram then represents an oblique section through the system of concentric cylinders described in the previous paragraph. The photographs show ellipses, the short axis of which is parallel to the line around which the powder sample has been rotated. The ellipses

are more or less elongated according to the angle of inclination of the sample. Each ellipse reproduces the intensity variation along the lines hk related by the pseudo-hexagonal symmetry between the level $Z=0$ (the small axis of the ellipse) and a maximum value of Z (the major axis of the ellipse). The perfection of orientation of the (001) faces of the particles is indicated here by the fineness of the ellipses. The particular value of this method is that it permits one to follow variations of $\sum |F_{hk}(Z)|^2$ up to large values of Z , of the order of 0.8 \AA^{-1} in reciprocal space. Secondary maxima of $\sum |F_{hk}(Z)|^2$ may be seen which never appear in X-ray diagrams because of the insufficient orientation of the material. The data obtained by oblique diffraction together with results obtained by the SAD technique provide valuable information for the ultimate refinement of the layer structure of smectites.

The preceding discussion concerns the turbostratic smectites, montmorillonite, hectorite, etc. In contrast to these, beidellite and saponite have three-dimensionally periodic structures. Some of these minerals can be disorganized by an appropriate dispersion (Weir, 1960; Weir and Greene-Kelly, 1962) and then they behave like turbostratic minerals. Some beidellite cannot be dispersed so completely and may remain in a crystalline state. The study of these three-dimensionally ordered minerals by electron diffraction involves the same considerations as those of other well-crystallized minerals such as kaolinite.

METHODS OF PREPARATION

Free particles dispersed in a suspension must be collected on a suitable substrate and must lie quite flat without being curved or folded. The first operation is to obtain a dispersion as complete as possible of the initially aggregated material. This requires consideration of the exchangeable cation. Ca-montmorillonite in water forms suspensions with very little stability which, after sedimentation in a thin layer, give films with poor orientation. This absence of orientation shows that the water has liberated relatively large flocculated particles which are not planar. The same operation applied to Na-montmorillonite produces very stable suspensions forming, after sedimentation, strongly oriented films. In this case the water has liberated much smaller planar elements and the free particles approximate more closely to the primary particles. This type of suspension is very suitable for studies by electron microscopy and diffraction, and in what follows, it will be understood that a suspension of a Na-smectite in pure water has been used.

Forming a deposit of free particles of a smectite gives rise to a new difficulty that is related to the mobility of these fine particles in suspension. The forces that hinder the dispersion of the particles are mainly edge-to-edge forces and these tend to produce edge-to-edge associations when a drop of a suspension is evaporated. Preparation techniques should be chosen so as to restrict this phenomenon of aggregation to a minimum; they should emphasize the attraction of the substrate for the particles over and above the

mutual interactions between the particles and the action of the interface between air and liquid. The most effective method is that of electrodeposition (Mering, Oberlin, and Villière, 1956). This is quite laborious and often can be replaced by immersing a copper grid covered with a carbon membrane in a dilute suspension. Deposition takes place as if the supporting membrane were positively charged by a difference of contact potential with respect to the metal grid. It has been checked that this technique fails for colloids which are positively charged, such as hydroxides. The same effect is produced when a drop of extremely dilute suspension of the order of parts per million, is deposited on the supporting membrane. In this case the attraction of the membrane collects all the particles before evaporation has had time to increase the concentration. With the two last techniques, it is never certain that edge-to-edge aggregation is eliminated completely, but it is reduced considerably. Finally with the three preceding techniques a flat deposit can be obtained and curving and folding of the particles is largely avoided. These techniques have been applied in the present studies.

For the HRD technique, the amount of material deposited by the techniques described above is insufficient. However, one must always avoid increasing the concentration of the suspension in order to increase the thickness of the deposit, since concentrated suspensions produce disoriented deposits. It is preferable to repeat deposition several times using drops of very dilute suspension.

ELECTRON MICROSCOPE STUDIES

Montmorillonite

Several varieties of montmorillonite are known to exist. The most common is represented by the montmorillonite from Camp-Berteaux, Morocco. Another variety occurring less frequently is represented by the Wyoming montmorillonite. These two varieties are not fundamentally different, either in chemical composition or structure, but differ mainly in their colloidal properties. Wyoming montmorillonite is much less sensitive to acid attack than the montmorillonites more generally found. There are differences also in the rheological properties of their stable suspensions. These properties are related to the dimensions of the primary particles and to their different modes of association in the free particles.

Montmorillonite from Camp-Berteaux.—This smectite, which is representative of most montmorillonites, is characterized by a tendency for the particles to show very strong edge-to-edge association which is more difficult to counteract than in other smectites.

The method of electrodeposition does not eliminate this effect unless applied for very short times. The particles then obtained have diameters of about 300 Å and are too small to be used with the SAD technique. Extending the period of electrodeposition leads to a growth of the apparent particle

diameter so that even with this technique edge-to-edge association is not eliminated. The equivalent of a moderate duration of electrodeposition is obtained by using extremely dilute drops (Plate 1). This photograph corresponds to a preparation suitable for SAD technique. Numerous complementary shapes are seen, marked by arrows in the photograph, of one aggregate adjacent to another. This leads one to think that large particles pre-existed in the suspension which were broken when attached to the substrate. However, this interpretation is contradicted by all other results obtained. For example, the diameters of the aggregates seen in Plate 1 increase with the concentration of the suspension in the drop and finally a continuous film is obtained. When a coarse fraction of sodium montmorillonite is used in place of a fine fraction, a film showing complementary contours is never obtained, and only membranes more or less folded and superposed are produced. The phenomena shown in Plate 1 correspond to a two-dimensional crystalline

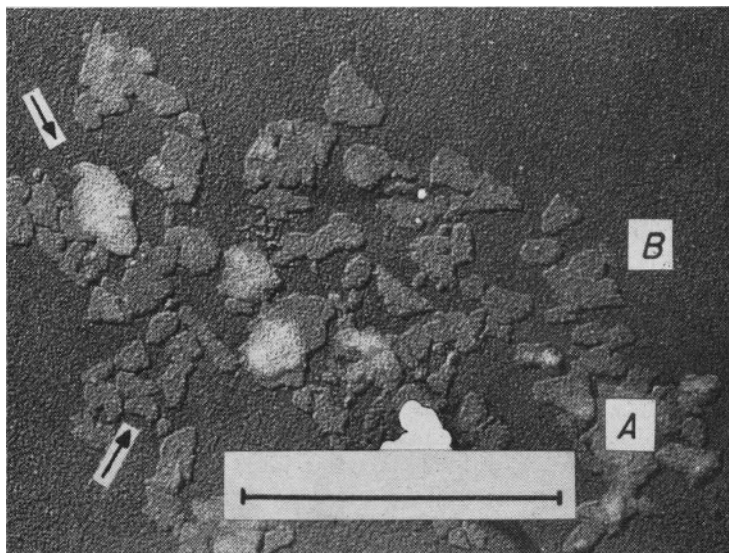


PLATE 1. Camp-Berteaux montmorillonite (Na)—fine fraction—dilute suspension (shadow cast with carbon).

growth taking place on the supporting substrate. The first two-dimensional aggregates formed are developed by new elements of very small size being added to the free edges of the aggregates. This growth is stopped in regions such as A marked in Plate 1 where the edges of adjacent aggregates approach so close to each other as to prevent the insertion of new elements. As in the growth of a crystalline nucleus, each supplementary element tends to be deposited on the edges of the aggregate but with a preference for positions

where the forces of interaction at the edges operated freely, for example at point B in Plate 1.

To summarize, the common form of montmorillonite, such as that from Camp-Berteaux, is characterized by strong interactions between edges related no doubt to strong edge charges. The nature of this interaction is shown by using exchange cations other than sodium. Deposits obtained from a dilute alkaline suspension rapidly converted into an acid suspension show almost total disappearance of edge-to-edge association (Mathieu-Sicaud *et al.*, 1951). When the same fresh acid suspension is partially saturated with calcium, the lateral growth is accelerated. The control obtained by the method of electrodeposition shows that this lateral growth is produced no longer on the supporting substrate but within the suspension. The effect of edge-to-edge association is emphasized here because it distinguishes the common type of montmorillonite from the less common type of Wyoming montmorillonite.

Montmorillonite from Wyoming.—This mineral is more easily studied in the electron microscope and special precautions to avoid edge-to-edge aggregation are not required. The methods of electrodeposition and of deposition from drops give the same results. In the latter method, the particle diameters are independent of solution concentration, and particles with complementary contours are never observed. Deposits obtained from acid suspensions with or without partial saturation with calcium produce the same results. Particles with diameters varying from 2000 Å to 5000 Å are observed and one finds they are deposited as flat forms (Plate 2*a*) showing occasionally a local fold (Plate 2*b*). This last phenomenon is an additional argument in favor of the pre-existence of the observed particles in the suspension.

Nontronite

Electron micrographs show elongated particles in the form of laths or in forms resembling that of montmorillonite. According to the origin of the mineral, either one or the other or both of these appear in a given specimen (Mackenzie, Meldau, and Robertson, 1952). The elongated form is the most frequent. Plates 3*a* and *b* are given by nontronite from Pfaffenreuth (Bavaria). The particles show little tendency for edge-to-edge association and, therefore, represent more or less faithfully the free particles in the suspension. Their average width is about 2000 Å. However, one cannot say whether the long ribbons folded perpendicular to their length are free particles or longitudinal associations (see the double arrows in the figure). With thick particles (Plate 3*b*) moiré fringes are frequently seen perpendicular to the length of the particles.

Hectorite

The most representative mineral of this species is that from Hector (Calif.) which is characterized by a strong tendency for edge-to-edge association of

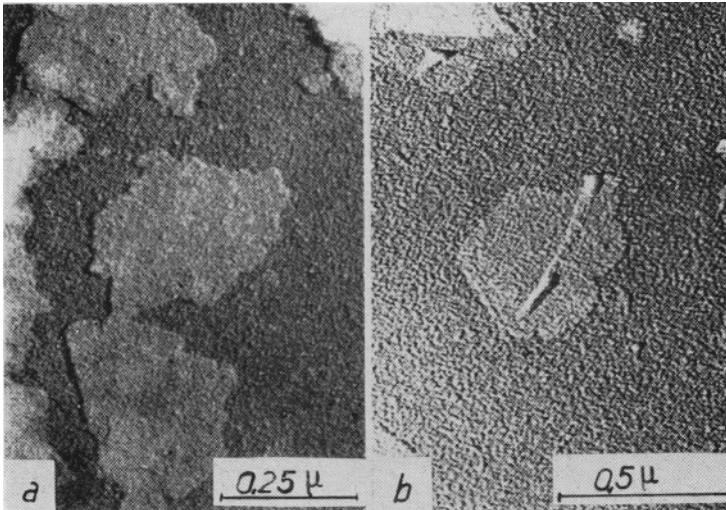


PLATE 2. Wyoming montmorillonite (Na), shadow cast with carbon: (a) flat particle, (b) distorted particle.

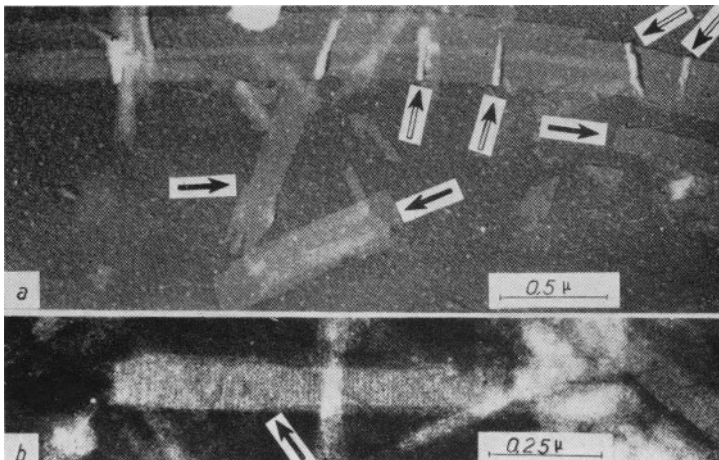


PLATE 3. Pfaffenreuth nontronite (Na), shadow cast with carbon: (a) thin particles, (b) moiré patterns in thick particles.

the particles like the montmorillonite from Camp-Berteaux though to a less degree. This is eliminated only by electrodeposition but is greatly reduced by using a drop of very dilute suspension. The free particles are in the form of laths more than 1 micron in length, with a width of about 1000 Å. Plates

4*a* and *b* show the main morphological characteristics; edge-to-edge associations are numerous and occur parallel to the length of the laths (Plate 4*a*) or at the extremities (Plate 4*b*, marked by arrow). In the first case, the contours are visible when the attachment is incomplete. In the second case, the particles make angles of 60° or 120° with each other due to the hexagonal outlines of the ends of the laths.

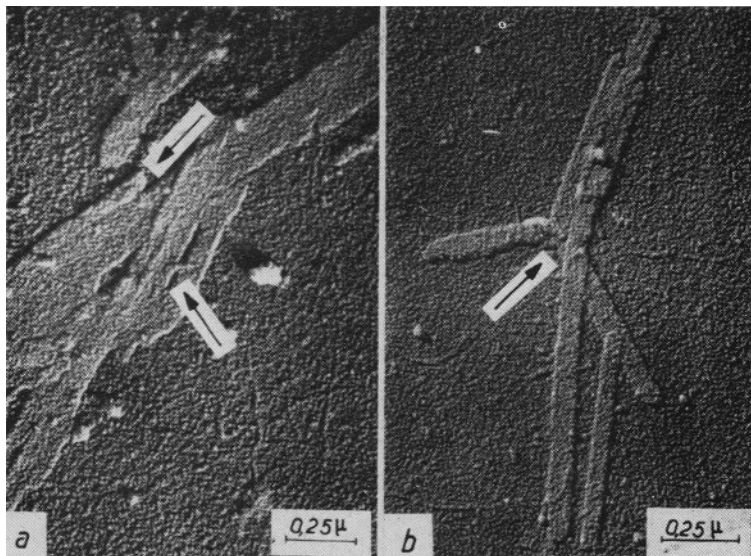


PLATE 4. Hectorite (Na). Shadow cast with carbon: (a) association edge-to-edge, (b) association at the ends of particles.

Comparison of the Four Species

The four species described fall into two groups according to their colloidal properties. Wyoming montmorillonite and nontronite exhibit no tendency for edge-to-edge association, and the observed particles are representative of the free particles in suspension.

In the Camp-Berteaux montmorillonite and probably in a majority of montmorillonites edge-to-edge association is especially strong and only a short period electrodeposition reveals the free particles; in all other cases, the observed particles are aggregates. In hectorite, the edge-to-edge association is less strong and isolated laths can be observed by all methods of sample preparation, including electrodeposition, so that the laths are regarded as free particles.

The edge interactions are considered to arise from edge charges and these must be considered as absent in Wyoming montmorillonite and Pfaffenreuth nontronite.

It is of interest to consider other physico-chemical properties. The nontronite and Wyoming montmorillonite take up a significant number of silanol groups that are measurable at high pH values (Glaeser and Mantin, 1967), whereas Camp-Berteaux montmorillonite and hectorite take up a negligible number. By a controlled acid attack on the Camp-Berteaux montmorillonite, measurable silanol groups can be obtained. Acid attack removes peripheral octahedral cations and leaves an edge of silica showing silanol groups. In the absence of such a silica boundary, the weak acidity of silanol groups is completely blocked by the strong acidity of the peripheral charges created by the Mg-for-Al substitutions. It is concluded that Wyoming montmorillonite and the Pfaffenreuth nontronite have a silica fringe naturally and consequently their edges have no exchange capacity.

SELECTED AREA DIFFRACTION (SAD) STUDIES

Thin Particles

Electron microscope observations of shadowed preparations show that particles not exceeding a single layer in thickness are of frequent occurrence. SAD diagrams of such monolayers have been sought but are difficult to obtain because non-shadowed specimens are used in order to avoid scattering by the shadowing material. In this case, one works "blind" and consequently in the field of observation there will often be more than one particle. Consequently, one must choose diagrams where the diffraction is dominated by a single particle, and it will be considered that the diagram is that of a single monolayer when such patterns can be repeated many times. It will be seen later that the diagrams given by thick particles produced by stacking of layers are quite different.

Montmorillonite from Camp-Berteaux (Oberlin and Mering, 1962).—SAD patterns record a section of reciprocal space at $Z=0$, which corresponds to a projection of the structure on its (001) plane and this can have a plane symmetry of $c2mm$, or $clm1$. For these two groups, only those intensities (hk) with $k=3n$ should give hexagonal symmetry. Plate 5 shows the SAD pattern of a monolayer of Camp-Berteaux montmorillonite. The entire diagram exhibits hexagonal symmetry. This also was shown in diagrams published by Cowley and Goswami (1961). It indicates that the particles are not truly monocrystalline, but are twinned by edge associations making angles of 60° and multiples of 60° , which alone can maintain the monocrystalline appearance of the diagram. Thus the SAD diagrams confirm what has been seen in the electron microscope and already described. It must then be concluded that the free particles seen after a short period of electrodeposition are still edge-to-edge associations of extremely small elements arranged with exactly 60° orientations.

Wyoming montmorillonite.—This mineral gives SAD diagrams where the intensities of certain (hk) spots, with $k \neq 3n$, do not show hexagonal symmetry.

Plate 6 shows the type of diagram obtained where the enhancement of 02 with respect to 11 is seen. The extinction of four spots of type 22, $\bar{2}2$ is observed, but the two spots 04 are seen, marked by arrows in the plate. These characteristics appear consistently for all thin particles and one can conclude that they are monocrystalline and consequently there is an identity between free particles and primary particles. Hence, there must be absence of edge-to-edge association in agreement with the electron microscope data.

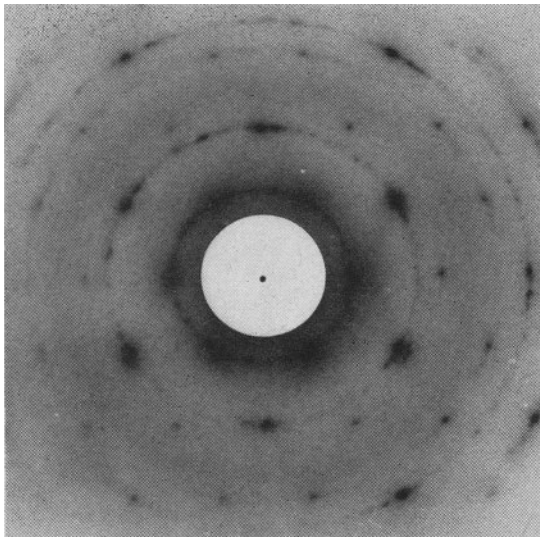


PLATE 5. SAD diagram for Camp-Berteaux montmorillonite (thin particle).

The SAD diagrams allow the true symmetry of the monocrystalline, two-dimensional layers to be determined. There exist three possibilities for arrangement of the Al ions in octahedral positions; a centro-symmetrical arrangement corresponds to the plane group $c2mm$ (analogous to $C2/m$ in three dimensions) and two equivalent non-centrosymmetrical arrangements corresponding to the plane group $c1m1$ (analogous to $C2$). The diffracted intensities at the level $Z=0$ calculated for the two arrangements are given in Table 1, columns 2 and 3. The observed intensities, estimated visually from the diagrams and photometered for the spots $0k$, are given in column 4, normalized with respect to 10 for 06, 33, since the intensities of this group are independent of the symmetry group.

It is to be noted that in these considerations, it is supposed that the particles are precisely oriented with (001) perpendicular to the electron beam. Any orientation other than 90° would mean that each reflection was recorded at a different level Z of reciprocal space. Calculation shows that interferences (hk) with $k=3n$ vary very rapidly with Z and consequently a variation of

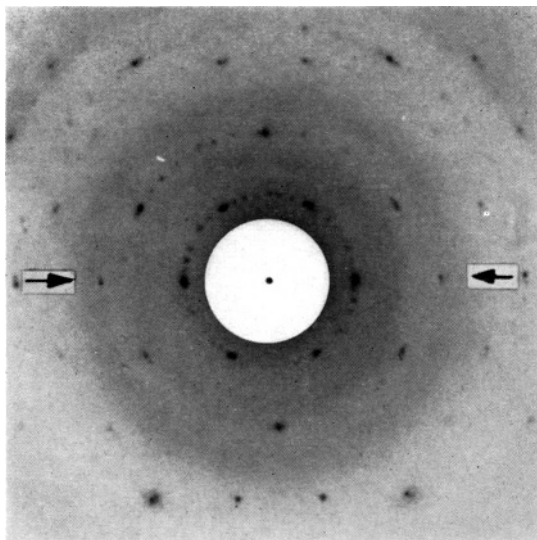


PLATE 6. SAD diagram for Wyoming montmorillonite (thin particle).

TABLE 1.—CALCULATED AND ESTIMATED INTENSITIES FOR MONTMORILLONITE

1	2	3	4
<i>hk</i>	<i>I</i> (calc) <i>c2mm</i>	<i>I</i> (calc) <i>clm1</i>	<i>I</i> (obs) (Wyoming)
02	16.0	6.8	7
11	0	4.8	5
20	1.2	1.2	4
13	1.2	1.2	4
04	0.3	2.0	2
22	1.2	0.3	0
24	0	0.8	1
15	0	0.8	1
31	3.0	1.4	2
06	10.0	10.0	10
33	10.0	10.0	10

orientation destroys the hexagonal symmetry of spots such as 20, 13 for example. Thus the hexagonal symmetry of hk spots with $k=3n$ constitutes a good check of the orientation of the particle with respect to the electron beam. This hexagonal symmetry of spots with $k=3n$ leaves only three sets of spots on which to base considerations of the layer symmetry.

Table 1 shows immediately that the symmetry group $cm1$ agrees better with the experimental data than $c2mm$. The set of spots 02, 11 is the most striking because it is the least dependent on deviations from the ideal model structure assumed in the calculations. Centro-symmetry requires complete extinction of the four 11 spots. The conclusion of non-centrosymmetry confirms the conclusion previously based on considerations of the solvation properties of bi-ionic montmorillonites of Na and Ca (Mering and Glaeser, 1954; Glaeser and Mering, 1954).

Nontronite (Pfaffenreuth).—The photographs obtained with thin particles are perfectly reproducible and correspond to diffraction by single monocrystalline layers (Plate 7). They show that the ribbons observed in the electron microscope are elongated parallel to the a -axis of the two-dimensional

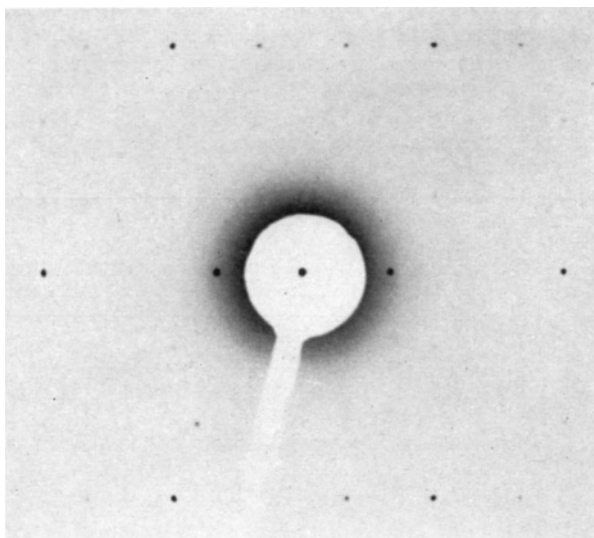


PLATE 7. SAD diagram for nontronite (thin particle).

crystal.* The monocrystalline appearance, analogous to that given by Wyoming montmorillonite, together with an absence of edge-to-edge association, suggest that most particles of the nontronite examined are both free particles and primary particles. Since nontronite is also dioctahedral, there is a question as to its true symmetry. Table 2 compares the calculated intensities for the symmetry groups $c2mm$ (col. 2) and $cm1$ (col. 3) with the observed intensities (col. 4). For the spots 02, 11 (whose intensities are insensitive to differences between the ideal structural model and the actual structure), nontronite appears to be a centro-symmetric structure; the

* This is shown by comparison of thin particle SAD patterns with the patterns of thick particles (see later) which are visible without shadowing.

observed intensities for 02, 11 are in good agreement with those calculated for the symmetry $c2mm$. This is contrary to the result found for montmorillonite.

For other spots, the discrepancies between observed and calculated data are considerable, and one concludes that the real structure of nontronite differs appreciably from the ideal model used in the calculations.

The structure model has been modified, therefore, along the lines indicated by the distortions found in muscovite (Radoslovich, 1960; Gatineau, 1963). A rotation of the SiO_4 tetrahedra by 12° around an axis through the Si atoms and normal to (001) has been used. The oxygen and (OH) positions in the octahedral layer have been modified so as to increase the size of the vacant octahedra, at the same time retaining the symmetry $c2mm$. The positions of the silicon and iron atoms have been kept unchanged. The intensities calculated with this modified model are given in Table 2, column 5. Agreement with the observed data is improved. This is only a first step towards the refinement of the structure, which should be taken further with the help of data obtained with the oblique HRD technique.

TABLE 2.—CALCULATED AND MEASURED INTENSITIES FOR NONTRONITE

1	2	3	4	5
<i>hk</i>	<i>I</i> (calc) <i>c2mm</i>	<i>I</i> (calc) <i>clm1</i>	<i>I</i> (obs) (Pfaffenreuth)	<i>I</i> (calc) <i>c2mm</i> modified structure
02	138	48	140	150
11	0	46	0	0
20	0	0	6	6
13	0	0	8	5
04	0	21	4	3
22	15	4	3	2
24	0	10	1	2
15	0	10	1	5
31	28	9	35	26
06	100	100	90	100
33	100	100	100	100

Hectorite (Oberlin and Mering, 1966).—The SAD diagram of a thin particle (single layer) is given in Plate 8. Again the elongation is parallel to the *a*-axis.*

In this case there is no symmetry problem because hectorite is trioctahedral. However, Plate 8 shows a striking anomaly; *hk* spots with $k=3n$

* See previous footnote.

differ considerably from hexagonal symmetry. Enhancement of the 13 and 26 spots are obtained in all diagrams. This symmetry anomaly for the 20, 13 and 40, 26 spots varies considerably from one SAD diagram to another, and also it is seen that when 13 and 26 are strongly enhanced, then the 06 spots are considerably diminished. This behaviour cannot be attributed to a discrepancy between the ideal model and the real structure. The anomalies can be understood better by considering X-ray diffraction data. The profile

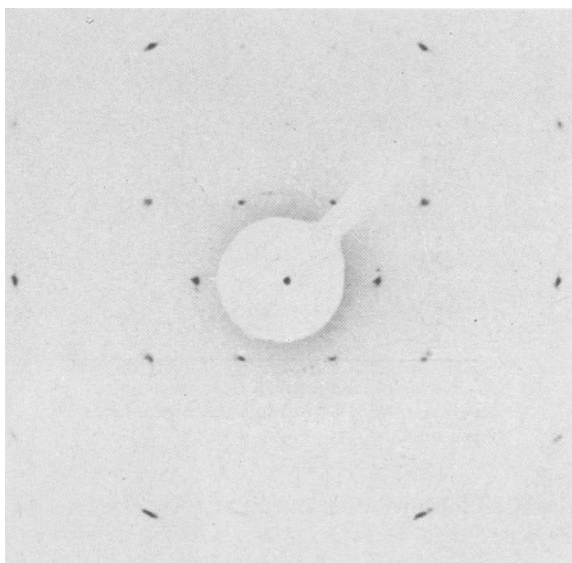


PLATE 8. SAD diagram for hectorite (thin particle).

of the X-ray diffraction band indicates a very considerable elongation of the primary particles in the a -direction, but does not allow a width greater than about 200 Å. Therefore, the free particles seen with a width of 1000 Å must be edge-to-edge associations of smaller elements joined by their sides parallel to a . An interpretation of the SAD patterns is obtained by supposing that the primary particles have variations of orientation around a . This means that only the 20 and 40 spots represent $|F^2|$ at the level $Z=0$. For all other spots, the recorded intensity is an integration along the Z direction, being greater when the k index is larger, i.e. when one is further away from the axis of rotation in the reciprocal space. The calculated intensities must depend on the angle of rotation that is chosen. For the lines 13 and 26 in reciprocal space, $|F_{hk}(Z)|^2$ grows rapidly with $|Z|$ away from $Z=0$. On the contrary, for lines 06, 33 the opposite variation is calculated. Therefore, it is seen that according to the extent of the rotation, 13 and 26 spots are reinforced while 06 is diminished. Table 3 compares the observed intensities found in Plate 8

TABLE 3.—CALCULATED AND
MEASURED INTENSITIES FOR
HECTORITE

<i>hk</i>	<i>I</i> (obs)	<i>I</i> (calc)*
02	71	69
11	28	21
20	8	6
13	16	18
04	3 ⁻	4
22	3 ⁺	4
24	7	7
15	5	8
31	14	14
06	66	73
33	80	92
40	14	14
26	24	47

* *I*(calc) assumes a variation of rotation of $\pm 8^\circ$ around the *a*-axis—see text.

with values calculated for a rotation of the primary particles by $\pm 8^\circ$ around the *a*-axis. The agreement is satisfactory. Likewise, a good agreement is obtained for other SAD patterns with appropriate choice of the rotation angle.

Thick Particles

Stacking of several layers gives similar results for all the smectites studied with the exception of Wyoming montmorillonite. The stacked layers are disoriented with respect to one another by rotation around an axis perpendicular to (001). This is limited and does not exceed about $\pm 10^\circ$. Plate 9 shows a stacking of two layers of nontronite and it is seen that the relative intensities from the two components remain the same. Plate 10 also for nontronite shows the result obtained with about twenty stacked layers. Plate 11 corresponds to a very thick particle of Camp-Berteaux montmorillonite.

Turbostratic disorder is always a rotational disorder, combined with a certain tendency for the layers to have a mutual orientation.

Thick particles of Wyoming montmorillonite show a different behaviour (see Plate 12). The turbostratic disorder is still one of rotation, but without any tendency for mutual orientation of the successive layers.

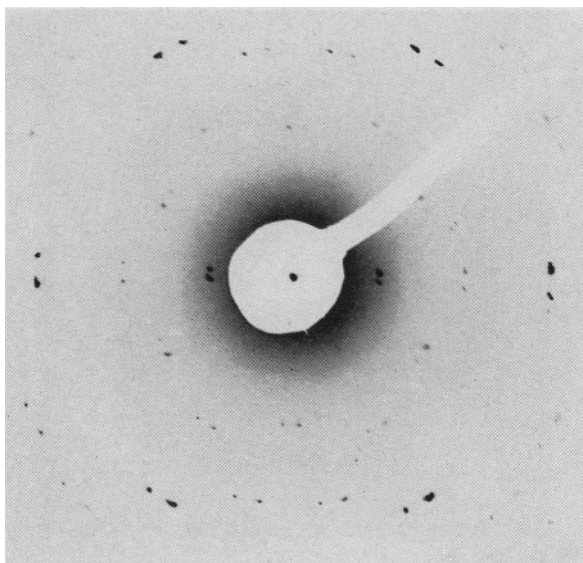


PLATE 9. SAD diagram for nontronite (two layers, thick particle).

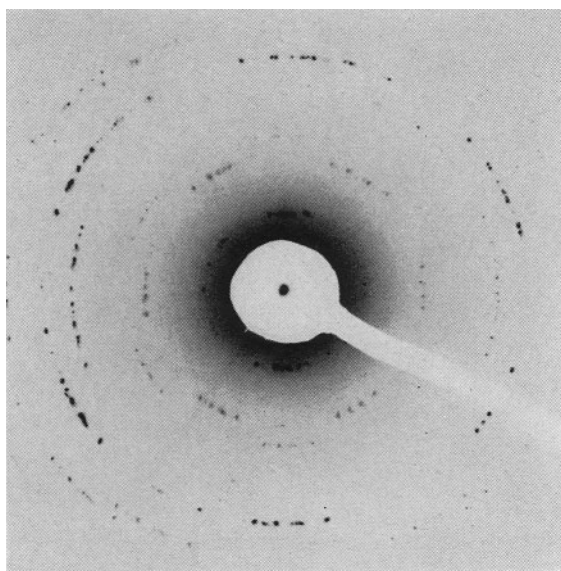


PLATE 10. SAD diagram for nontronite (thick particle).

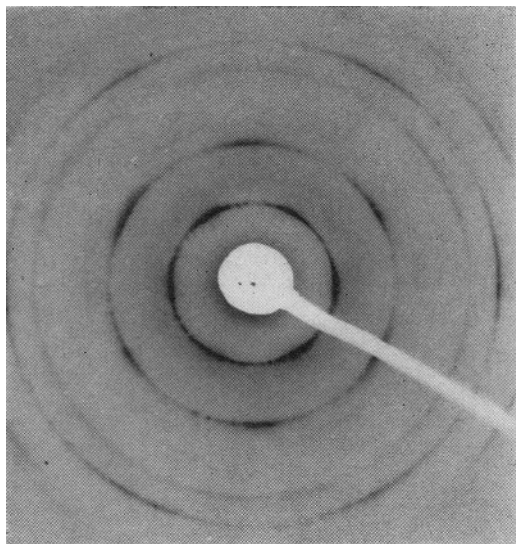


PLATE 11. SAD diagram for Camp-Berteaux montmorillonite (very thick particle).

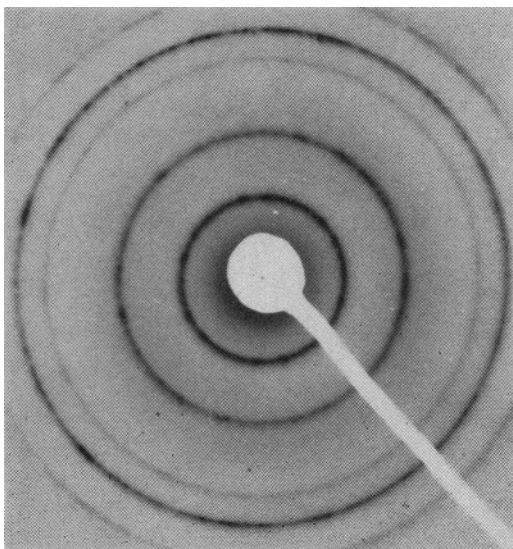


PLATE 12. SAD diagram for Wyoming montmorillonite (very thick particle).

Conclusions from SAD Studies

The combined use of SAD technique and the electron microscope has shown that, in the case of Camp-Berteaux montmorillonite and of hectorite, even the free particles forming a monolayer are not truly monocrystalline. Each layer is an edge-to-edge association of much smaller primary particles. In montmorillonite this association occurs with orientations defined as a multiple of 60° . In hectorite, it occurs parallel to the length and has fluctuations of orientation around this direction. The layers of Wyoming montmorillonite and of nontronite are single two-dimensional crystals, the symmetry groups of which have been determined.

The SAD patterns of monolayers of montmorillonite and nontronite show that the real structures are somewhat disordered with respect to the ideal structures. The refinement of the structure analysis cannot be completed with the limited data furnished by the SAD technique, but must be completed with the help of the HRD oblique method.

HIGH RESOLUTION DIFFRACTION (HRD) DATA

Sample Perpendicular to Electron Beam

This method gives precise unit cell parameters. The results are as follows:

montmorillonite (Wyoming and Camp-Berteaux) $b=9.02 \pm 0.02 \text{ \AA}$,

nontronite (Pfaffenreuth and Limousin) $b=9.18 \pm 0.04 \text{ \AA}$,

hectorite (Hector) $b=9.09 \pm 0.02 \text{ \AA}$.

The relation $b=a\sqrt{3}$ is always obtained thanks to the fineness of the rings observed in these diagrams.

Oblique Sample Method

In the oblique diagram of a three-dimensionally periodic phyllite, all the ellipses carry intensity maxima which can be seen particularly at large values of Z . These maxima are hkl reflections. Plate 13 gives the diagram of a beidellite from Rupsroth, whose state of order has been established by X-rays (Hofmann *et al.*, 1956; Weir, 1960). Table 4 indicates the positions of the reflections according to the value of Z , in \AA^{-1} , in reciprocal space. These maxima are specially sharp and numerous on the ellipse $20l$, $13l$, and their positions agree with the unit cell determined by Zvyagin and Pinsker (1949) for a specimen of askanite with $c=9.95 \text{ \AA}$ and $\beta=100^\circ$. It is probable that the specimen examined by these authors was a beidellite.

In a turbostratic smectite the ellipses show fewer and more diffuse maxima which represent simply the variations of $|F_{hk}(Z)|^2$ along the corresponding reciprocal lattice line.

Complete calculations have been made for the case of hectorite (Oberlin and Mering, 1966) the diagram of which is given in Plate 14. On the line 20 , 13 are two maxima, partially separated, for $Z=0.46 \text{ \AA}^{-1}$ and $Z=0.61 \text{ \AA}^{-1}$, which agree in position, intensity, and shape with the maxima of the function

TABLE 4.—OBLIQUE TEXTURE PATTERN OF BEIDELLITE; OBSERVED VALUES OF $Z \text{ \AA}^{-1}$ FOR VARIOUS hkl REFLECTIONS

$02l, 11l$	$20l, 13l$	$04l, 22l$
—	0.13	
0.19		
0.23		
0.27	0.26	0.28
	0.31	
		0.33
	0.44	
	0.51	
	0.61	
	0.83	

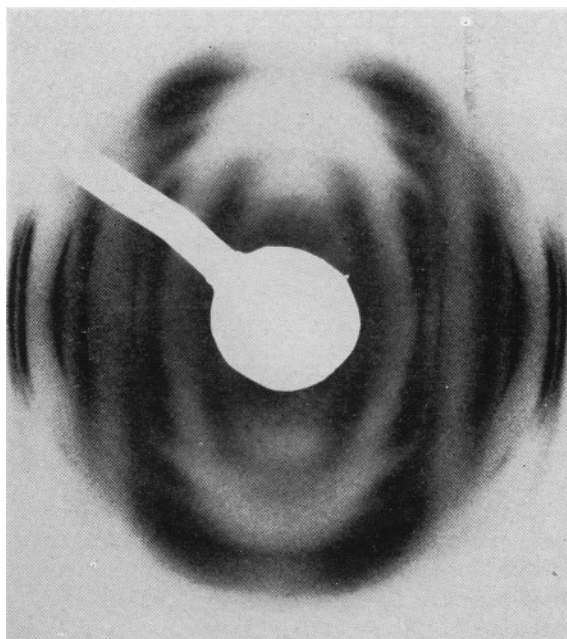


PLATE 13. Oblique texture pattern of Rupsroth beidellite.

$\sum |F_{hk}(Z)|^2$ calculated for the ideal model of the mineral. An equally good agreement is obtained for the line 40, 26. This shows that the structure of hectorite approaches the ideal model. The non-distortion of this structure must be related to its trioctahedral character and the fact that the substituting cations (Li) have the same radius as Mg.

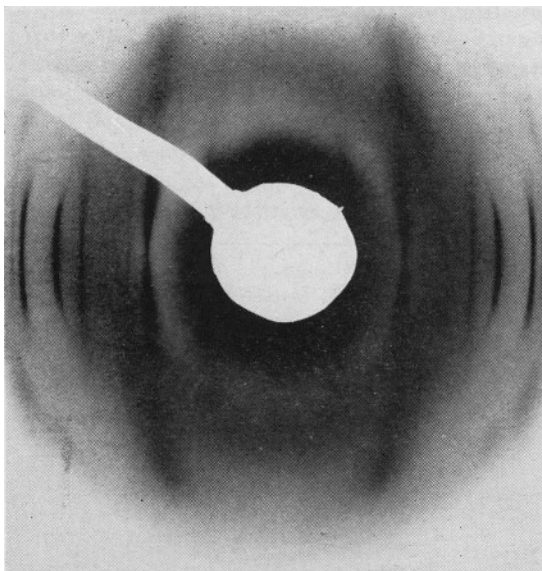


PLATE 14. Oblique texture pattern of hectorite (tilt angle 65°).

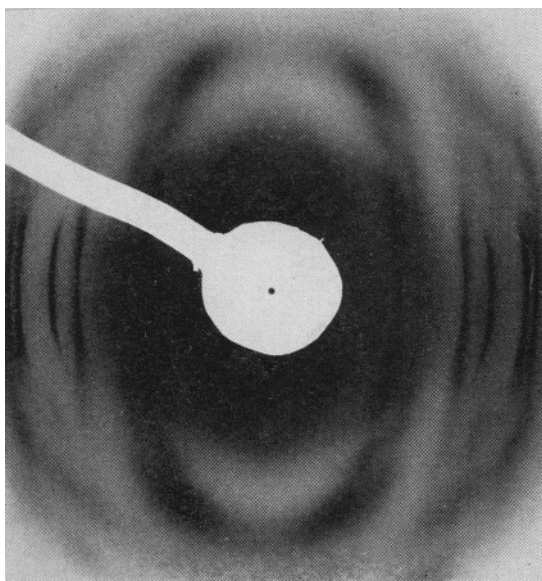


PLATE 15. Oblique texture pattern of Wyoming montmorillonite (tilt angle 60°).

2

The case of montmorillonite is less simple because SAD has shown a certain disagreement between the ideal and the real structure; the observed 20, 13 intensities are stronger than the calculated values. The oblique diagrams (Plate 15) show intensity maxima on the 20, 13 and 40, 26 lines which are separated better than those of hectorite.

TABLE 5.—COMPARISON BETWEEN $\sum |F_{hk}(Z)|^2$ AND EXPERIMENTAL RESULTS FOR 20, 13 IN MONTMORILLONITE

$Z \text{ \AA}^{-1}$ (calc)	$Z \text{ \AA}^{-1}$ (mcas)	I (calc)	I (obs)
min 0.36	min 0.36	8	zero
max 0.48	max 0.44	50	weak
min 0.58	min 0.53	17	zero
max 0.66	max 0.59	33	strong

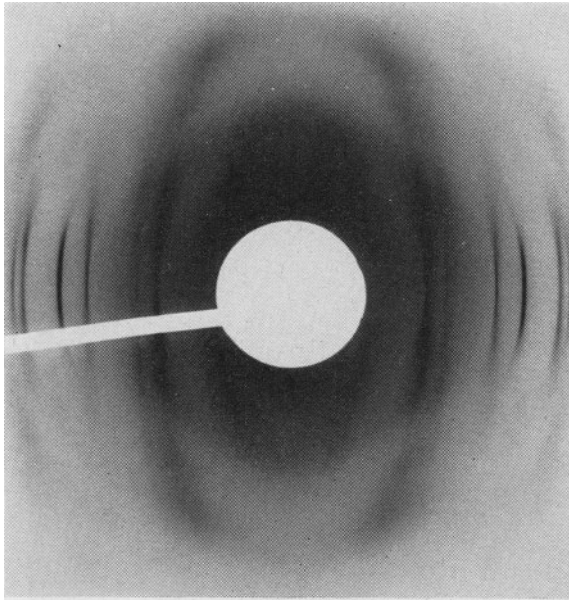


PLATE 16. Oblique texture pattern of nontronite (tilt angle 65°).

The montmorillonites from Camp-Berteaux and from Wyoming give identical diagrams. The calculated form of the function $\sum |F_{hk}(Z)|^2$ shows maxima of similar width to those observed, but their position and intensity do not agree with the observed data. This disagreement is seen in Table 5 for the larger values of $Z \text{ \AA}^{-1}$. It is concluded that the observed maxima

follow the fluctuations of $\sum |F_{hk}(Z)|^2$ but the real structure is far from the ideal model used in the calculations.

The diagram of nontronite, Plate 16, is very similar to that of montmorillonite but is more diffuse. It shows a similar disagreement between the experimental results and those calculated from the ideal model.

The last two smectites are at present the subject of a tentative structure refinement. It is apparent that oblique diagrams are sensitive to distortions of the ideal structures, and may provide a method for obtaining more exact structural data.

REFERENCES

- BRINDLEY, G. W., and MERING, J. (1951) Diffraction des rayons X par les structures en couches désordonnées: *Acta Cryst.* **4**, 441-7.
- COWLEY, J. M., and GOSWAMI, A. (1961) Electron diffraction patterns from montmorillonite: *Acta Cryst.* **14**, 1071-9.
- GATINEAU, L. (1963) Localisation des remplacements isomorphiques dans la muscovite: *C.R. Acad. Sci.* **256**, 4648-9.
- GLAESER, R., and MANTIN, I. (1967) *Bull. Soc. Franç. Minér. Crist.* In press.
- GLAESER, R., and MERING, J. (1954) Isotherme d'hydratation des montmorillonites bi-ioniques: *Clay Miner. Bull.* **2**, 188-93.
- HOPMANN, U., WEISS, A., KOCH, G., MEHLER, A., and SCHOLZ, A. (1956) Intracrystalline swelling, cation exchange and anion exchange of minerals of the montmorillonite group: *Clays and Clay Minerals*, Proc. 4th Conf., Natl. Acad. Sci.—Natl. Res. Council Pub. 456, 273-87.
- MACKENZIE, R. C., MELDAU, R., and ROBERTSON, R. H. S. (1952) Teilchenform und Mineralogie einiger Nontronite: *Ber. Deutsch. Keram. Gesell.* **29**, 221-6.
- MATHIEU-SICAUD, A., MERING, J., and PERRIN BONNET, I. (1951) Étude au microscope électronique de la montmorillonite et de l'hectorite: *Bull. Soc. Franç. Minér. Crist.* **74**, 439-56.
- MERING, J., and GLAESER, R. (1954) Rôle de la valence des cations échangeables dans la montmorillonite: *Bull. Soc. Franç. Minér. Crist.* **77**, 519-30.
- MERING, J., OBERLIN, A., and VILLIÈRE, J. (1956) Étude par électro-déposition de la morphologie des montmorillonites: *Bull. Soc. Franç. Minér. Crist.* **79**, 515-22.
- OBERLIN, A., and MERING, J. (1962) Microscopie et micro-diffraction électroniques sur la montmorillonite: *Jour. microscopie, France* **1**, 107-20.
- OBERLIN, A., and MERING, J. (1966) Observations sur l'hectorite: *Bull. Soc. Franç. Minér. Crist.* **89**, 29-40.
- RADOSLOVICH, E. W. (1960) The structure of muscovite: *Acta Cryst.* **13**, 919-32.
- WEIR, A. H. (1960) Study in the relationship between certain physical properties and structure and composition of montmorillonite group minerals: Ph.D. Thesis, University of London. (Rothamsted Exper. Sta., Harpenden.)
- WEIR, A. H., and GREENE-KELLY, R. (1962) Beidellite: *Amer. Min.* **47**, 137-46.
- ZVYAGIN, B. B. (1957) Étude des minéraux argileux en diffraction électronique: *Rev. Étude et Emploi Argiles* (Université Lvov) May-June, 769-75.
- ZVYAGIN, B. B., and PINSKER, Z. G. (1949) Structure of montmorillonite: *C.R. Acad. Sci. URSS.* **68**, 65-7, and 505-8.